Composites Part B 103 (2016) 131–138

Contents lists available at ScienceDirect

Composites Part B

journal homepage: www.elsevier.com/locate/compositesb

Short-term creep of barkcloth reinforced laminar epoxy composites

Samson Rwawiire [a, b, *], Blanka Tomkova [a], Jakub Wiener [a], Jiri Militky [a], Allan Kasedde [b], Bandu M. Kale [a], Abdul Jabbar [a]

[a] Department of Material Engineering, Technical University of Liberec, Studentská 2, 461 17 Liberec, Czech Republic
[b] Department of Textile and Ginning Engineering, Busitema University, P.O Box 236, Tororo, Uganda

ARTICLE INFO

Article history:
Received 18 May 2016
Received in revised form
31 July 2016
Accepted 17 August 2016
Available online 20 August 2016

Keywords:
Barkcloth
Creep
Mechanical properties
DMA

ABSTRACT

There is a global surge in the application of natural fiber reinforced polymer composites in various industries. Polymer reinforced composites are faced with dimensional instability during their service life, the reason being that the realistic environment of application has got frequency and temperature variables. Therefore, in order to pinpoint the dimensional stability of the composites, creep tests are usually carried out. In this investigation, for the first time, alkali, enzyme, and plasma treated barkcloth reinforced epoxy laminar composites were investigated using dynamic mechanical analysis for the creep behavior between the temperature range of 30 °C–100 °C. The results show that creep is affected by the layering pattern of the laminar composites whereas alkali treatment leads to a higher creep resistance of the composites.

© 2016 Elsevier Ltd. All rights reserved.

1. Introduction

The global impact of the consequences of climate change due to an increase in greenhouse gas emissions are visible. Synthetic fibers whose main feedstock is petroleum, contribute to environmental degradation due to the toxicity of the fumes emitted, demanding energy for production and their non-biodegradability. Various regional, national and international legislations have led to a worldwide push for reduction in green house gas emissions in transportation and manufacturing industries through utilization of sustainable and renewable materials [1–3]. Lignocellulosic fibers on the other hand have various advantages such as: biodegradability, high specific strength, low energy demands and are readily available [4–7]. Barkcloth is a lignocellulosic nonwoven fabric majorly made up of cellulose (69%) and produced from the bark of *Ficucs natalensis* and *Antiaris toxicaria trees* which are widely grown in Central Uganda [8]. Research elsewhere showed that barkcloth can be used as a reinforcement of polymer composites and the fabric also has robust sound absorption properties at higher frequencies [9,10]. Treatment of barkcloth fabrics with enzyme and plasma had a positive effect on the properties of the fabrics. Enzyme treatment had a positive effect in dissolving of plant material, hemicelluloses and lignin; consequently leading to enzyme treated fabrics being thermally stable whereas treatment with plasma led to the excitation of the reactive sites of cellulose [11]. Alkali treatment dissolved hemicelluloses, lignin and plant material leading to an increase in the strength of barkcloth; Alkali-treated fabrics were used to reinforce commercially available green epoxy polymer; the produced composites had enough strength for interior automotive panels [12].

In the recent years, fiber reinforced polymer composites from renewable resources have found applications in various industries, however, because polymers and polymer composites are viscoelastic in nature among the tests performed to ascertain the dimensional stability of the developed materials is creep [13]. Creep is the time dependent behavior of a material whereby a constant stress is applied to a material and the resulting strain is characterized. The study of polymer composites necessitates the evaluation of the viscoelastic behavior of the composites at various frequencies and temperature. The viscoelastic behavior is best demonstrated using creep and stress relaxation tests; one such tool that can be used is in the evaluation of the creep behavior of polymer composites is the Dynamic Mechanical Analysis [14].

Synthetic fiber reinforced polymer composites are used in the construction industry for rehabilitation of structures [15]. Mancusi et al. studied carbon and glass laminar composites retrofitted PC beams whereby carbon and glass fiber composite laminates were bonded by adhesives on to the beams and the structures subjected to creep experimental tests at room temperature. The retrofitted

* Corresponding author. Department of Textile and Ginning Engineering, Faculty of Engineering, Busitema University, P.O Box 236, Tororo, Uganda.
E-mail address: rsammy@eng.busitema.ac.ug (S. Rwawiire).

http://dx.doi.org/10.1016/j.compositesb.2016.08.027
1359-8368/© 2016 Elsevier Ltd. All rights reserved.

structures were creep resistant at low stress levels whereas at high stress levels, there was change in mechanical response of the structures which was due to the localized stresses in the adhesive materials [16]. Furthermore, various models aimed at creep analysis of rehabilitated civil engineering structures have been reported [17,18].

Previous investigation on the creep of natural fibrous reinforced composites shows that creep is dependent on the temperature, types of matrix, filler pre-treatment and the filler type and size [19–21].

There are limited studies of the creep behavior of barkcloth reinforced composites; therefore a detailed critical analysis of creep of barkcloth composites is of practical importance. The objectives of this study are therefore: (1) investigate the short-term creep behavior of barkcloth reinforced laminar epoxy composites. (2) Understand the effect of fabric pre-treatment with enzyme, plasma and alkali on the creep behavior. (3) Study the effect of advanced layering architecture on the creep behavior of barkcloth composites.

2. Experimental

2.1. Materials

Barkcloth from *Ficus natalensis* was extracted using the method described by Rwawire et al. [12]. An overview of barkcloth material and mechanical properties is shown in Table 1 [8,22,23] and Table 2 [8,12]. Two commercially available enzymes "Texazym DLG", "Texazym BFE", and anti-foaming agent "Texawet DAF" supplied by inoTEX spol. s.r.o, Czech Republic were utilized as described elsewhere [11]. Two sets of epoxy resin were utilized: Synthetic Epoxy resin LG285 and amine hardener HG 285 supplied by GRM systems, Czech Republic; Green epoxy CHS-Epoxy G520 which is a biodegradable low molecular weight basic liquid epoxy resin containing no modifiers, certified by the International Environmental Product Declaration Consortium (IEC). The green epoxy was utilized for the production of biocomposites (green composites).

Table 1
Overview of barkcloth material properties [8,18,19].

Property	Unit	Value
Physical and mechanical properties		
Areal weight (Alkali Treated)	g/m^2	142
Areal weight (Untreated)	g/m^2	327
Average thickness	mm	1.12
Fabric strength		
Microfiber bundle Direction	N	101.7
Transverse	N	23.5
Chemical composition		
α-Cellulose	%	68.69
Hemicellulose	%	15.07
Lignin	%	15.24
Thermo-physiological properties		
Thermal conductivity coefficient	W/m K	0.0357
Thermal absorptivity	$Ws^{1/2}/m^2K$	0.197
Thermal resistance	m^2K/W	81.4
Thermal diffusivity	m^2s^{-1}	0.034
Peak heat flow density	$[Wm^2] \times 10^{-3}$	0.234
Relative water vapor permeability	%	66
Evaporation resistance	$Pa.m^2$	4.4

2.2. Fabric surface modification

2.2.1. Enzyme treatment

DLG enzyme was used together with BFE to form a mixture. The enzyme solution and fabric weight ratio was all throughout maintained at 1:30. 0.3 g of DLG and 0.6 g of BFE were added in 900 ml of distilled water. 0.2 g/l of Texawet DAF which is an anti-foaming agent was added and the mixture was conditioned at 55 °C ensuring a neutral pH for 90 min. Another bath was prepared using BFE enzyme with the same bath ratio above of 1:30. 0.6 g of the enzyme was mixed with the anti foaming agent and the bath maintained at 55 °C with for 90 min. An alkali was added so as to set the pH to 9. Caution was taken such that both enzymes are not heated with a direct heat source.

2.2.2. Plasma treatment

Barkcloth fabrics were treated with Dielectric Barrier Discharge (DBD) plasma using laboratory device, Universal Plasma Reactor 100 W, model FB-460, Class 2.5 from Czech Republic. The barkcloth fabric samples were put in the reactor for the duration of 30s and 60s respectively.

2.2.3. Alkali treatment

Barkcloth fabrics were subjected to alkali treatment of 5% NaOH solution. The barkcloth fabrics were soaked in an alkaline solution at room temperature for one hour thereafter thoroughly cleaned using distilled water to remove the alkali together with other impurities and then dried in an oven at 80 °C.

2.3. Composite fabrication

2.3.1. Synthetic epoxy composite

Vacuum Assisted Resin Transfer Molding (VARTM) was used to prepare the Barkcloth Fabric Reinforced Plastic Composites (BFRP). The resin to hardener ratio was 100:40 as per the manufacturer's specifications. The composites produced with VARTM had a 40% fiber volume fraction. Four barkcloth plies were used for the composite sample preparation for each set of composites (Fig. 1). After the resin infusion, the composite was left to cure at room temperature for 72 h.

Table 2
Summary of the barkcloth composite mechanical properties [8,12].

Laminar composites/property	Ultimate tensile strength [MPa]	Tensile modulus [GPa]	Flexure [MPa]	Flexural modulus [GPa]	Elongation [%]
Untreated	25–31	3.2–3.3	40–142	1.6–2.1	1.5
Plasma treated 30s	28–30	2.1–3.9	87–94	2.5–2.7	1.31
Plasma treated 60s	25–35	3.2–4.7	97–105	2.0–2.3	1.2–1.3
Enzyme treated (DLG)	15–18	0.58–2.5	37–49	1.6–1.9	0.9
Enzyme treated (BFE)	17–18	2.5–2.7	49–62	2.2–2.7	0.9
BFRP I	18–26	3.7–5.3	85–87	1.8–2.3	1.2–1.5
BFRP II	21–25	3.2–3.5	189–195	1.8–2.4	1.3
BFRP III	19–28	4.1–4.2	103–136	2.3–3.7	0.6–1.5
BFRP IV	24–27	3.2–4.9	130–175	2.3–3.5	0.8–2.1
Green composites	30–38	2.4–3	189–227	1.1–1.8	2.1–2.5

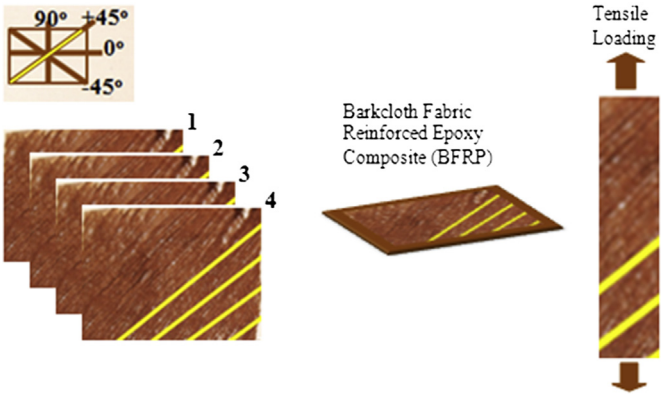

Fig. 1. Barkcloth plies and experimental loading.

2.3.2. Layered composites

Laminar hierarchical architecture was utilized with untreated (BFRP) and Biocomposites (green composites). Optimization of the fiber properties was achieved through varying the fiber angles through the hierarchical architecture of the barkcloth layers. The layering pattern of the barkcloth fabrics used for the purpose of the study of the effect of layering pattern is as shown in Fig. 2 as reported elsewhere [8].

2.3.3. Green epoxy composite

The biocomposite specimens were prepared using the hand lay-up due to the fact that the viscosity of the green epoxy polymer was high [12]. The mould was treated with a mould release agent and thereafter Teflon sheets were applied to aid the fast removal of cured composite specimens.

2.4. Characterization methods

2.4.1. Morphology

The surface morphologies were investigated using a TS5130 Vega-Tescan scanning electron microscope with accelerating voltage of 20 KV. The samples were sputtered with gold using a plasma sputtering device.

2.4.2. Fiber orientation distribution

In order to effectively determine the barkcloth fabric hierarchical architecture, a Hough Transform image analysis code was utilized.

2.4.3. Creep

The Creep behavior of BRPC was investigated using the three point bending (3 PB) mode utilizing a Texas Instruments Q800 Dynamic Mechanical Analysis (Q800 DMA) (Fig. 3). The short term creep tests were carried out in the viscoelastic region of the composites below the glass transition temperature. Synthetic Epoxy

Layering Sequence

Composites	Ply arrangement [°]
BFRP I	-45, 45, 0, 90
BFRP II	45, -45, 90, 0
BFRP III	0, 90, 45, -45
BFRP IV	90, 0, -45, 45

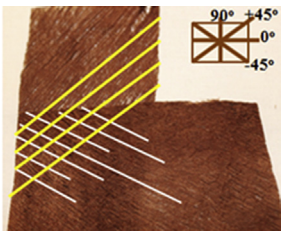

Fig. 2. Barkcloth Fabric Reinforced Plastic Composites (BFRP) layering sequence.

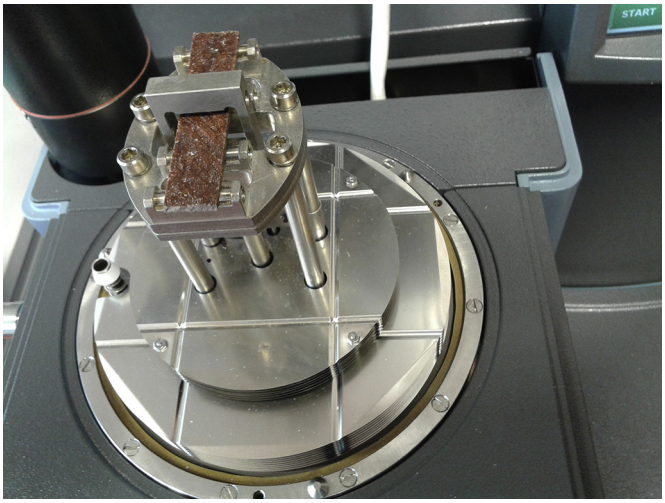

Fig. 3. Creep specimen mounted in 3PB jaws.

Composites (Untreated; Enzyme and Plasma Composites) were tested in the temperature range 50–60 °C whereas green epoxy polymer reinforced composites were tested in the temperature range 50–80 °C below the glass transition temperature. The samples with length and width dimensions of 60 × 12 mm and thickness ranging from 2 to 3 mm were equilibrated for 5 min at the set temperature; thereafter a static stress of 2 MPa was applied in three point bending mode for a period of 30min. The strain was measured using a high resolution linear optical encoder with a resolution of 1 nm that allows measuring displacements of very small amplitudes [24].

3. Results and discussion

3.1. Fiber orientation distribution

Image processing techniques are used in the microstructure investigation of nonwoven fabrics so as to understand fiber orientation distribution and fiber diameter. The Fourier Transform (FT), Hough Transform (HT) and Direct Tracking are the methods used in the estimation of the fiber orientation distribution in nonwoven materials [25]. Unlike other methods, the HT method obtains the fiber distribution in the nonwoven directly and the actual orientation of the straight lines is plotted on the image with minimal computational power. Using a digital camera image as shown in Fig. 4, it's observed that the bonded barkcloth microfiber bundles are nearly aligned at an angle of ±45° to the horizontal. These fiber bundles are held together through fiber entanglement. That notwithstanding, a robust technique utilizing the HT was further

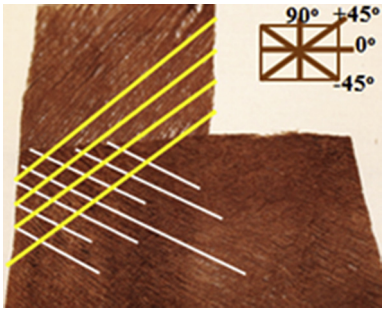

Fig. 4. Barkcloth ply angles.

used to investigate the microfiber bundle orientation distribution (Fig. 5). While using the HT, the image magnification affects the results obtained, elsewhere, Ghassemieh [26] showed that a magnification of 30× and 50× produced the best representative image of the nonwoven; consequently, the results were favorable compared to higher magnifications.

The 50× SEM image magnification was therefore utilized for image processing in matlab (Fig. 5A). In order for the HT to function optimally, the image was binarized (Fig. 5B); therefore the HT algorithm identifies points in the image which fall on to the straight lines. The lines are thereafter plotted on the original image. Fig. 5C shows the orientation of the most microfiber bundles in the barkcloth. The application of the HT further justifies the barkcloth microfiber bundle orientation of ±45°.

3.2. Fabric morphology

In our earlier research elsewhere, we extensively reported on the morphology of barkcloth [11,12,22,23]. It was shown that the fabric morphology is made up of a dense network of naturally bonded microfibers that are oval in shape with diameters 10–20 μm. The microfiber bundles appeared to be aligned at angles; the inter-fiber bond structure is responsible for the strength of the load bearing microfibers and damage is a result of the separation of the individual microfiber bundles through the failure of the inter-fiber bond and thence fracture. The transverse section of the fabric was typically characterized by air cavities and microfibers surrounded by plant material; It's the air cavities that are responsible for the thermal insulation and sound absorption properties of the fabric [10]. The morphology of enzyme and plasma treated fabrics is shown in Fig. 6. Plasmas are used for the surface activation of fibrous network and therefore depending on the treatment time, the material can have structural changes [27]. Fig. 6a and b are the SEM images of plasma treated fabrics for 30s and 60s respectively. It was observed that oxygen plasma had a slight effect on the surface of the barlcloth microfibers. The plant materials on the surface are vividly visible. Fig. 6c and d shows the effects of BFE enzyme treated fabrics whereas 6e and 6f are for DLG enzyme treated fabrics. Treatment of barkcloth with commercial enzyme BFE led to ridges and grooves along the microfibers surfaces (Fig. 6d). At 100× magnification, it wasn't possible to see the difference of enzyme treated barkcloth surfaces (Fig. 6c and e); that notwithstanding, an increase of magnification showed that the performance of BFE enzyme in dissolving plant material was better than DLG enzyme and the surfaces are fairly cleaner compared to the DLG enzyme (Fig. 6f).

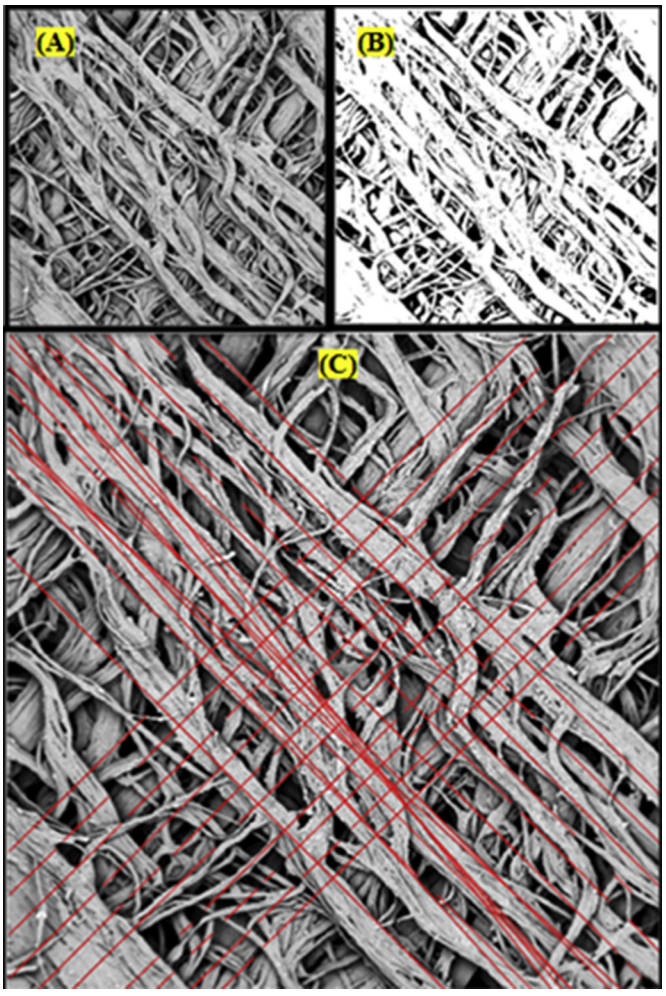

Fig. 5. Barkcloth fiber orientation distribution.

Fig. 7 shows the X-ray Diffraction pattern of barkcloth. The untreated barkcloth showed main 2θ diffraction peaks between 22.8° and 23.2° which correspond (002) crystallographic planes of cellulose I [28]. The peak at 15.3° is due to 001 crystallographic plane of cellulose I [29]. The crystalline index was calculated using the expression by Ref. [30] shown below:

$$CI = \frac{H_{22.55} - H_{18.5}}{H_{22.55}} \quad (1)$$

where $H_{22.55}$ is the height of the XRD peak at $2\theta = 22.55°$ which is responsible for both amorphous and the crystalline fractions whereas the small peak at $2\theta = 18.5°$ corresponds to the amorphous fraction. The calculated crystallinity index was 79% higher than sisal (71%), jute (71%), Sansevieria cylindria leaf fibers (60%) [31]. A higher value of CI shows that barkcloth crystallites are orderly in nature. Having orderly cellulose polymer crystallites aides in the resistance of the mobility of the cellulose polymer chains as temperature increases therefore making the reinforcement efficient.

3.3. Thermal behavior of biocomposites

The composites' thermal behavior as characterized by DSC is shown in Fig. 8. Incorporation of barkcloth into the amine hardener - epoxy polymer resin system had an effect on the crystallization behavior of semi-crystalline synthetic epoxy polymer. The barkcloth reinforced epoxy laminar composites experienced endothermic and exothermic phase transformation. The first endothermic peak at around 55–61 °C corresponds to the glass transition temperature (T_g) whereas a broad exothermic peak at around 133–150 °C represents the cold crystallization temperature (T_c) of the epoxy polymer chains [32]. As the temperature is increased, a second endothermic peak is observed at around 200–220 °C. This peak signifies the melting temperature (T_m) of Epoxy polymer. Table 3 shows the effect of surface modification of barkcloth on the T_g, T_c and T_m. Addition of reinforcement generally increased the glass transition temperature, crystallization temperature as well as the melting temperature of the composites because addition of reinforcement limits the mobility of the polymer chains and therefore, a positive effect on the glass transition temperature [33]. In comparison to enzyme treatment, plasma treated barkcloth had a higher glass transition temperature0.

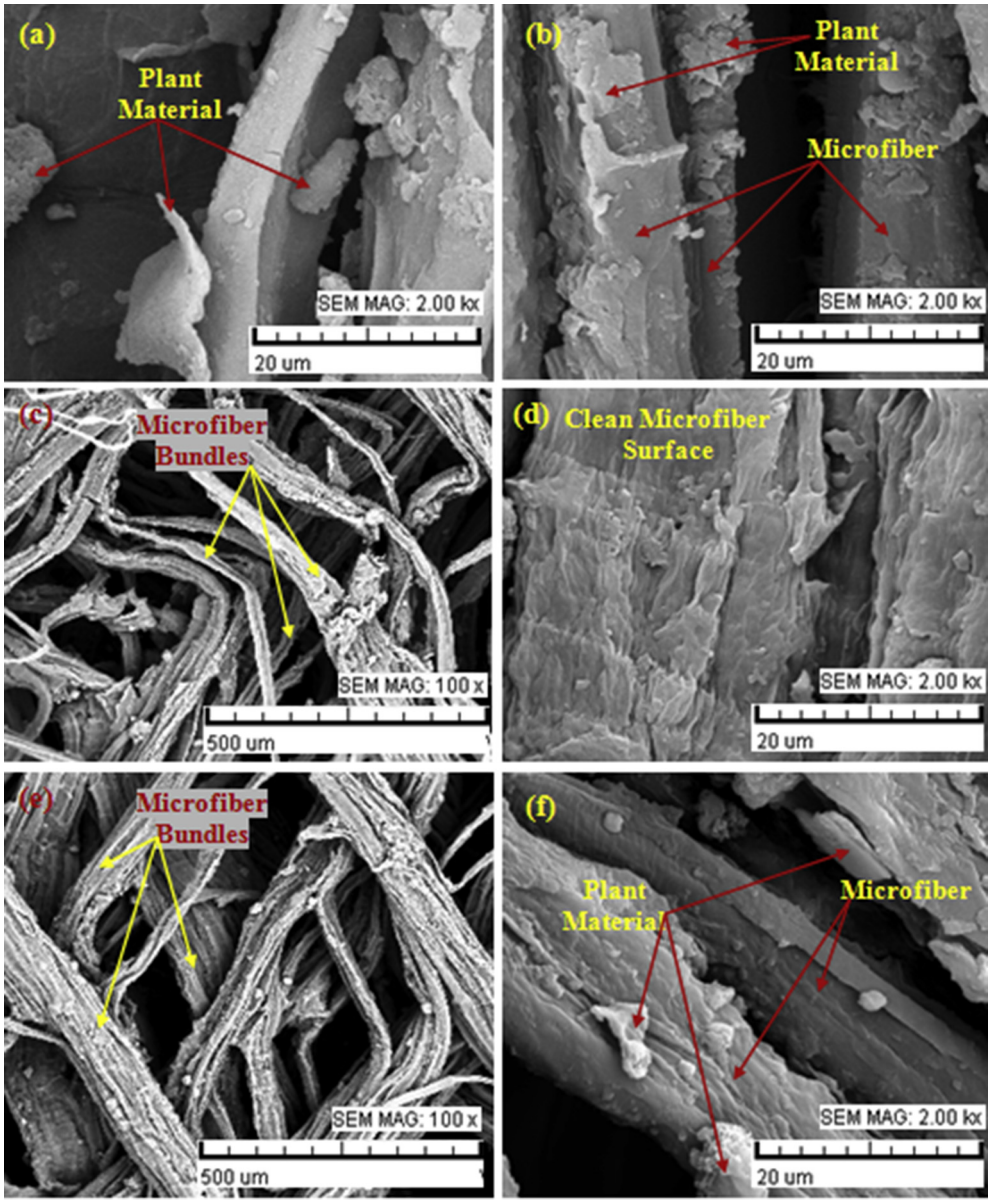

Fig. 6. Enzyme and Plasma Treated Barkcloth Fabric Morphology: (a) Plasma 30s; (b) Plasma 60s; (c) BFE enzyme treated surface view of fabrics; (d) BFE enzyme treated microfiber surface view (e) DLG enzyme treated surface view of fabrics (f) DLG enzyme treated microfiber surface view.

3.4. Dynamic mechanical properties

In order to evaluate the effect of the surface modification, the mechanical damping factor (Tan δ) was utilized to show the efficiency of the surface modified filler-matrix adhesion. A high damping factor indicates a weak filler-matrix adhesion, whereas a low damping factor indicates good filler-matrix adhesion that doesn't allow free movement of polymer molecules. It's therefore observed that plasma treated composites for 60s and enzyme treated composites had good fiber-to-matrix adhesion as can be observed by the lower Tan δ (Table 4). The glass transition temperature is obtained at the level at which the damping factor and loss modulus attain maximum damping values [34]. Table 4 shows the three temperature ranges of glass transition obtained using the loss modulus curve; peak of damping factor and by DSC respectively. The glass transition obtained using tan δ is usually higher; therefore, a more conservative glass transition temperature obtained by the loss modulus is usually taken into consideration.

Creep behavior is characterized by three stages: decreasing strain rate, stable strain rate and an increasing strain rate [21]. The creep resistance test results were obtained from the Texas Instruments Q800 Dynamic Mechanical Analyzer and the data of barkcloth fabric reinforced composites in the temperature range of 30–80 °C was plotted as shown in Figs. 9, 10, 11 and 12 respectively. The composites were all still in the stable strain rate at the end of the tests. Overall, it was observed that the untreated composites had low instantaneous deformation and the lowest creep rate at both the temperatures which were studied. The instantaneous deformation of the untreated fabrics gradually increased with increase in temperature. The lowest resistance to creep was observed with DLG enzyme treated fabric composites at both temperatures of the test. The low creep resistance is due to the action of enzymes which dissolved the plant material and weakened the fabric inter-fiber bonds therefore leading to weaker composite structures. However, that notwithstanding, despite the fact that overall enzyme treated composites had the highest creep rate, an increase

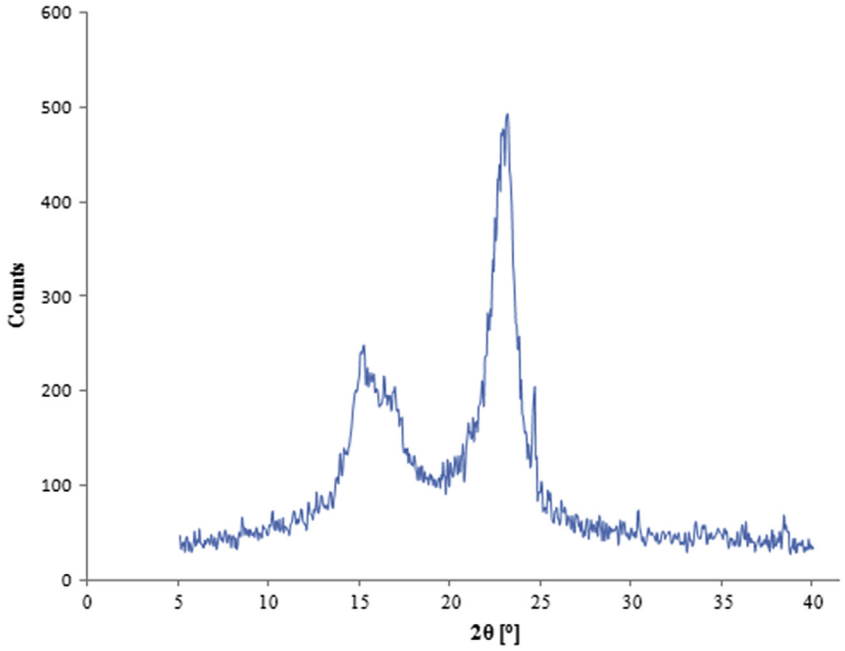

Fig. 7. X-ray diffraction of barkcloth.

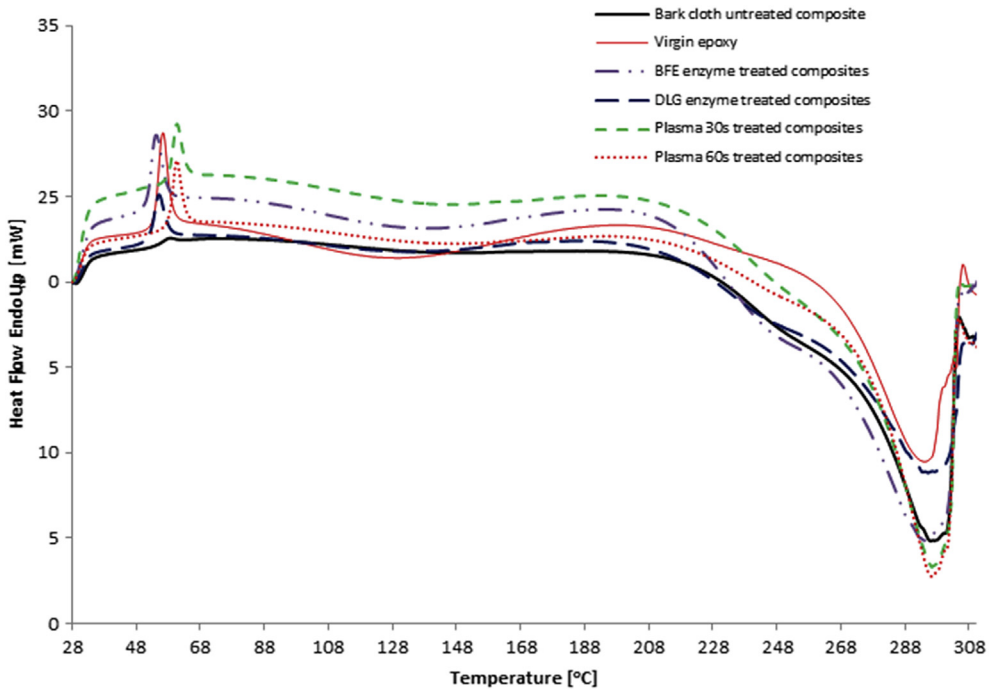

Fig. 8. Differential Scanning Calorimetry (DSC) behavior of composites reinforced with enzyme.

Table 3
DSC of BFRP.

Composites	T_g [°C]	T_c [°C]	T_m [°C]
Untreated	59	141	220
Virgin epoxy	56	133	200
BFE composites	55	140	210
DLG composites	56	137	206
Plasma 30s composites	61	146	213
Plasma 60s composites	61	150	215

in temperature from 30 °C to 50 °C had little effect on the creep behavior of BFE enzyme treated fabric reinforced composites. The effect of layering pattern on the creep of Barkcloth Fabric Reinforced Plastic Composites (BFRP) was investigated as shown in Figs. 11 and 12. It's observed that layering pattern BFRP II had a low instantaneous deformation and higher creep resistance at both the tested temperatures being closely followed by BFRP IV. This behavior is consistent with the results obtained for the flexural and dynamic mechanical properties reported elsewhere therefore giving proof that advanced hierarchical ply arrangement BFRP II and IV

Table 4
Dynamical mechanical properties of composites.

Composites	Storage modulus [GPa]	T_g [°C] (peak of loss modulus curve)	T_g [°C] (peak of tan δ curve)	T_g [°C] (DSC)	Peak value of tan δ
Untreated	8.04	59.4	66.4	59	0.54
DLG composites	7.20	57.5	61.8	56	0.49
BFE composites	3.38	53.7	59.7	55	0.50
Plasma 60s	8.54	54.9	62.2	61	0.51
Plasma 30s	8.04	57.2	69.0	61	0.54

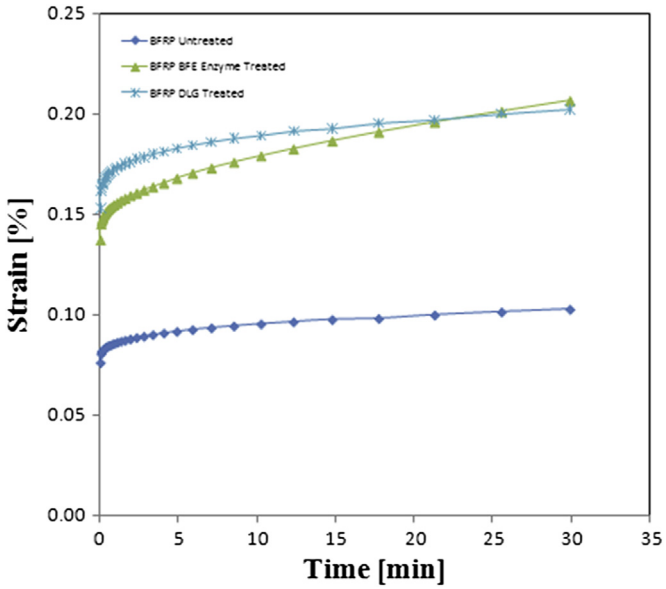

Fig. 9. Creep behavior of Enzyme treated Composites at 30 °C.

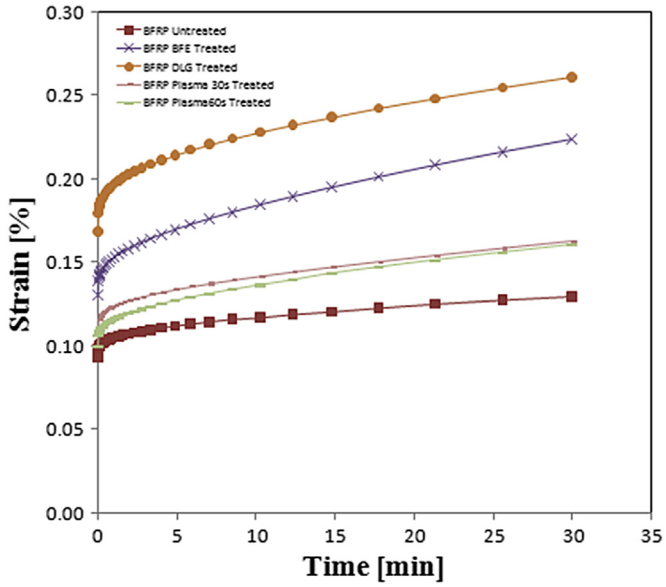

Fig. 10. Creep behavior of Enzyme and Plasma treated Composites 50 °C.

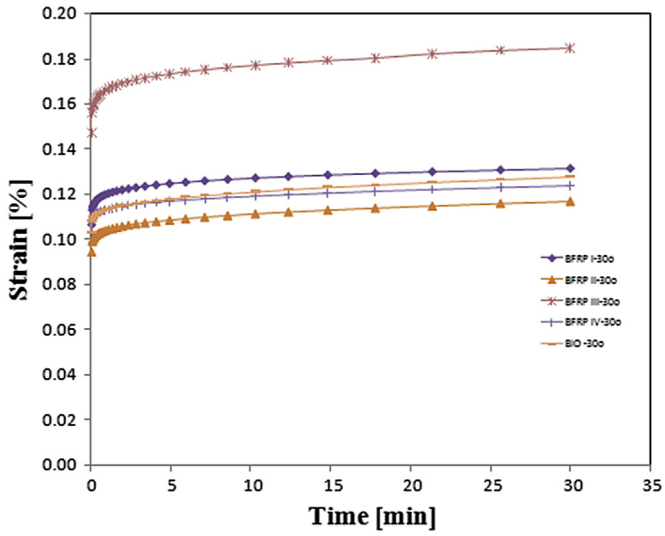

Fig. 11. Effect of layering pattern on Creep behavior of Synthetic and green composites at 30 °C.

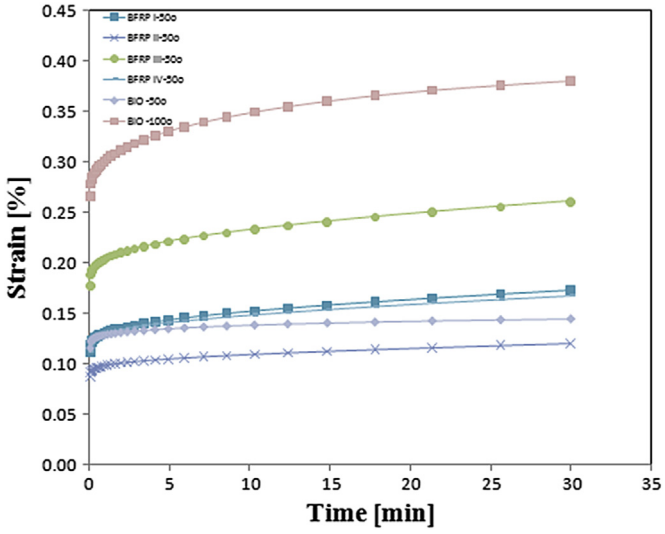

Fig. 12. Effect of layering pattern on Creep behavior of Synthetic and green composites at 50 °C and 100 °C.

being ideal for barkcloth composite laminate design [8]. The green composites utilized layering sequence BFRP IV; at 30 °C the composites creep behavior is almost the same with synthetic composites with the same ply arrangement, however, as the temperature increases to 50 °C (Fig. 12), the green composites' creep resistance wasn't affected by temperature change therefore showing the green epoxy polymer's creep resistance being higher than the synthetic composites with the same layering pattern. This result was due to the effect of treatment of the fabrics with alkali which increased the crystalline nature of the reinforcing fabric and also to the crystallinity of the green epoxy polymer. However, that notwithstanding at a higher temperature of 100 °C, the green composites exhibited a very low creep resistance which would render the optimum temperature of application of the green composites with barkcloth reinforcement lower than 100 °C. In

order to harness the best composite mechanical properties, barkcloth fabrics, layering sequence BFRP II and IV are therefore recommended to be used, whereas alkali treatment is preferred and yields better static and dynamic mechanical properties.

4. Conclusion

We investigated the short-term creep behavior of barkcloth reinforced laminar epoxy composites; the effect of fabric pretreatment with enzyme, plasma and alkali on the creep behavior and finally the effect of advanced layering architecture on the creep behavior of barkcloth composites was studied. Untreated barkcloth composites have a very low instantaneous deformation. Enzyme treated fabric reinforced fabrics had a very low creep resistance however an exception was seen with BFE enzyme treated composites which were not affected by temperature change. The effect of layering on the creep behavior showed that layering sequence II (Barkcloth Fabric Reinforced Plastic Composites, BFRP II) had the lowest creep rate as well as having the lowest instantaneous deformation. Treatment with alkali not only improves the mechanical properties but it also renders the alkali treated composites resistant to creep within the 30–50 °C temperature range. The optimum temperature of operation of the green composites should be below 100 °C.

Acknowledgments

The first author is grateful to God for life; to the Association of African Universities (AAU) for funding the Research; Technical University of Liberec (TUL) for the Ph.D study scholarship and Busitema University for granting the study leave.

References

[1] Alves C, Ferrão PMC, Silva AJ, Reis LG, Freitas M, Rodrigues LB, et al. Ecodesign of automotive components making use of natural jute fiber composites. J Clean Prod 2010;18:313–27. http://dx.doi.org/10.1016/j.jclepro.2009.10.022.
[2] Faruk O, Bledzki AK, Fink H-P, Sain M. Progress report on natural fiber reinforced composites. Macromol Mater Eng 2014;299:9–26. http://dx.doi.org/10.1002/mame.201300008.
[3] Change TIP on C. IPCC Fifth Assessment report. 2014.
[4] Mishra S, Mohanty AK, Drzal LT, Misra M, Hinrichsen G. A review on pineapple leaf fibers, sisal fibers and their biocomposites. Macromol Mater Eng 2004;289:955–74. http://dx.doi.org/10.1002/mame.200400132.
[5] Dittenber DB, Gangarao HVS. Critical review of recent publications on use of natural composites in infrastructure. Compos Part A Appl Sci Manuf 2012;43:1419–29. http://dx.doi.org/10.1016/j.compositesa.2011.11.019.
[6] Nabi Saheb D, Jog JP. Natural fiber polymer composites: a review. Adv Polym Technol 1999;18:351–63. http://dx.doi.org/10.1002/(SICI)1098-2329(199924)18:4<351::AID-ADV6>3.0.CO;2-X.
[7] Summerscales J, Dissanayake NPJ, Virk AS, Hall W. A review of bast fibres and their composites. Part 1 – fibres as reinforcements. Compos Part A Appl Sci Manuf 2010;41:1329–35. http://dx.doi.org/10.1016/j.compositesa.2010.06.001.
[8] Rwawiire S, Tomkova B, Militky J, Kale BM, Prucha P. Effect of layering pattern on the mechanical properties of bark cloth (*Ficus natalensis*) epoxy composites. Int J Polym Anal Charact 2015;20:160–71. http://dx.doi.org/10.1080/1023666X.2015.988534.
[9] Rwawiire S, Tomkova B. Static and dynamic mechanical properties of barkcloth (Ficus natalensis) -reinforced epoxy composite. J Nat Fibers 2016:0478. http://dx.doi.org/10.1080/15440478.2014.984061.
[10] Rwawiire S, Tomkova B, Gliscinska E, Krucinska I. Investigation of sound absorption properties of bark cloth. Autex Res J 2015:15. http://dx.doi.org/10.1515/aut-2015-0010.
[11] Rwawiire S, Tomkova B, Weiner J, Militky J. Effect of enzyme and plasma treatments of bark cloth from Ficus natalensis : morphology and thermal behavior. J Text Inst 2015:5000. http://dx.doi.org/10.1080/00405000.2015.1055989.
[12] Rwawiire S, Tomkova B, Militky J, Jabbar A, Kale BM. Development of a biocomposite based on green epoxy polymer and natural cellulose fabric (bark cloth) for automotive instrument panel applications. Compos Part B Eng 2015;81:149–57. http://dx.doi.org/10.1016/j.compositesb.2015.06.021.
[13] Georgiopoulos P, Kontou E, Christopoulos A. Short-term creep behavior of a biodegradable polymer reinforced with wood-fibers. Compos Part B Eng 2015;80:134–44.
[14] Jabbar A, Militký J, Kale BM, Rwawiire S, Nawab Y, Baheti V. Modeling and analysis of the creep behavior of jute/green epoxy composites incorporated with chemically treated pulverized nano/micro jute fibers. Ind Crops Prod 2016;84:230–40.
[15] Ascione L, Berardi VP, Aponte AD. Composites : Part B Long-term behavior of PC beams externally plated with prestressed FRP systems : a mechanical model. Compos Part B 2011;42:1196–201. http://dx.doi.org/10.1016/j.compositesb.2011.02.023.
[16] Mancusi G, Spadea S, Berardi VP. Composites : Part B Experimental analysis on the time-dependent bonding of FRP laminates under sustained loads. Compos Part B 2013;46:116–22. http://dx.doi.org/10.1016/j.compositesb.2012.10.007.
[17] Ascione L, Berardi VP, D'Aponte A. A viscoelastic constitutive law for FRP materials. Int J Comput Methods Eng Sci Mech 2011;12:225–32.
[18] Cricrı G, Perrella M, Calı C. An advanced creep model allowing for hardening and damage effects. Strain 2010:347–57. http://dx.doi.org/10.1111/j.1475-1305.2009.00682.x.
[19] Militký J, Jabbar A. Comparative evaluation of fiber treatments on the creep behavior of jute/green epoxy composites. Compos Part B Eng 2015;80:361–8.
[20] Xu Y, Wu Q, Lei Y, Yao F. Creep behavior of bagasse fiber reinforced polymer composites. Bioresour Technol 2010;101:3280–6.
[21] Wang W, Huang H, Du H, Wang H. Effects of fiber size on short-term creep behavior of wood fiber/HDPE composites. Polym Eng Sci 2015;55:693–700.
[22] Rwawiire S, Luggya GW, Tomkova B. Morphology, thermal, and mechanical characterization of bark cloth from Ficus natalensis. ISRN Text 2013:2013.
[23] Rwawiire S, Tomkova B. Thermo-physiological and comfort properties of Ugandan barkcloth from Ficus natalensis. J Text Inst 2014:1–6. http://dx.doi.org/10.1080/00405000.2013.843849.
[24] http://www.tainstruments.com/pdf/brochure/dma.pdf.
[25] Pourdehyhimi B, Dent R, Jerbi A, Tanaka S, Deshpande A. Measuring fiber orientation in nonwovens part V: real webs. Text Res J 1999;69:185–92.
[26] Ghassemieh E, Acar M, Versteeg H. Microstructural analysis of non-woven fabrics using scanning electron microscopy and image processing. Part 1: development and verification of the methods. Proc Inst Mech Eng Part L J Mater Des Appl 2002;216:199–207.
[27] Zille A, Oliveira FR, Souto AP. Plasma treatment in textile industry. Plasma Process Polym 2015;12:98–131.
[28] Madhukar B, Jakub K, Militky J, Rwawiire S, Mishra R, Jabbar A. Dyeing and stiffness characteristics of cellulose-coated cotton fabric. Cellulose 2016. http://dx.doi.org/10.1007/s10570-015-0847-0.
[29] Madhukar B, Wiener J, Militky J, Rwawiire S, Mishra R, Jacob KI, et al. Coating of cellulose-TiO 2 nanoparticles on cotton fabric for durable photocatalytic self-cleaning and stiffness. Carbohydr Polym 2016;150:107–13. http://dx.doi.org/10.1016/j.carbpol.2016.05.006.
[30] Segal L, Creely JJ, Martin AE, Conrad CM. An empirical method for estimating the degree of crystallinity of native cellulose using the X-ray diffractometer. Text Res J 1959;29:786–94.
[31] Sreenivasan VS, Somasundaram S, Ravindran D, Manikandan V, Narayanasamy R. Microstructural, physico-chemical and mechanical characterisation of Sansevieria cylindrica fibres – an exploratory investigation. Mater Des 2011;32:453–61. http://dx.doi.org/10.1016/j.matdes.2010.06.004.
[32] Hardis R, Jessop JLP, Peters FE, Kessler MR. Cure kinetics characterization and monitoring of an epoxy resin using DSC, Raman spectroscopy, and DEA. Compos Part A Appl Sci Manuf 2013;49:100–8. http://dx.doi.org/10.1016/j.compositesa.2013.01.021.
[33] Kim H. Enhancement of thermal and physical properties of epoxy composite reinforced with basalt fiber. Fibers Polym 2013;14:1311–6.
[34] Zhou F, Cheng G, Jiang B. Effect of silane treatment on microstructure of sisal fibers. Appl Surf Sci 2014;292:806–12. http://dx.doi.org/10.1016/j.apsusc.2013.12.054.